

Modeling maximum astrophysical gravitational recoil velocities

Carlos O. Lousto and Yosef Zlochower

*Center for Computational Relativity and Gravitation,
School of Mathematical Sciences, Rochester Institute of Technology,
78 Lomb Memorial Drive, Rochester, New York 14623*

(Dated: November 13, 2021)

We measure the recoil velocity as a function of spin for equal-mass, highly-spinning black-hole binaries, with spins in the orbital plane, equal in magnitude and opposite in direction. We confirm that the leading-order effect is linear in the spin and the cosine of angle between the spin direction and the infall direction at merger. We find higher-order corrections that are proportional to the odd powers in both the spin and cosine of this angle. Taking these corrections into account, we predict that the maximum recoil will be $3680 \pm 130 \text{ km s}^{-1}$.

PACS numbers: 04.25.dg, 04.30.Db, 04.25.Nx, 04.70.Bw

I. INTRODUCTION

The field of Numerical Relativity (NR) has progressed at a remarkable pace since the breakthroughs of 2005 [1–3] with the first successful fully non-linear dynamical numerical simulation of the inspiral, merger, and ringdown of an orbiting black-hole binary (BHB) system. BHB physics has rapidly matured into a critical tool for gravitational wave (GW) data analysis and astrophysics. Recent developments include: studies of the orbital dynamics of spinning BHBs [4–11], calculations of recoil velocities from the merger of unequal mass BHBs [12–14], and very large recoils acquired by the remnant of the merger of two spinning BHs [8, 15–29], empirical models relating the final mass and spin of the remnant with the spins of the individual BHs [30–37], and comparisons of waveforms and orbital dynamics of BHB inspirals with post-Newtonian (PN) predictions [38–45].

The surprising discovery [15, 16] that the merger of binary black holes can produce recoil velocities up to 4000 km s^{-1} , and hence allow the remnant to escape from major galaxies, led to numerous theoretical and observational efforts to find traces of this phenomenon. Several studies made predictions of specific observational features of recoiling supermassive black holes in the cores of galaxies in the electromagnetic spectrum [46–52] from infrared [53] to X-rays [54–56] and morphological aspects of the galaxy cores [57–59]. Notably, there began to appear observations indicating the possibility of detection of such effects [60–62], and although alternative explanations are possible [63–66], there is still the exciting possibility that these observations can lead to the first confirmation of a prediction of General Relativity in the highly-dynamical, strong-field regime.

Numerical simulations of the BHB problem have sampled the parameter space of the binary for different values of the binary’s mass ratio q and arbitrary orientations of the individual spins of the holes. Two astrophysically important regions of this parameter space remain challenging to describe accurately by numerical simulations: the small q limit, although recent development

of the numerical techniques have produced a successful simulation of the last few orbits before the merger of a $q = 1/100$ binary [67], and the near maximal spin limit. The most recent simulations of highly-spinning BHBs was of non-precessing binaries with intrinsic spins $\alpha = 0.95$ [68]. Since BHBs with $\alpha = 1$ are still elusive to full numerical simulations, and the configuration that maximizes the gravitational recoil is one that starts with maximally spinning BHs, with opposite spins lying on the orbital plane [15, 16], we will model these configurations for different values of the intrinsic spin parameter up to $\alpha = 0.92$ (which is achievable with current techniques to solve initial “puncture” data) and then extrapolate to $\alpha = 1$ using an improved version of our original empirical formula [15, 16, 30].

In Ref. [30] we extended our original empirical formula for the recoil velocity imparted to the remnant of a BHB merger [15, 16] to include next-to-leading-order corrections, still linear in the spins. The extended formula has the form:

$$\begin{aligned} \vec{V}_{\text{recoil}}(q, \vec{\alpha}) &= v_m \hat{e}_1 + v_{\perp} (\cos \xi \hat{e}_1 + \sin \xi \hat{e}_2) + v_{\parallel} \hat{n}_{\parallel}, \\ v_m &= A \frac{\eta^2 (1-q)}{(1+q)} [1 + B \eta], \\ v_{\perp} &= H \frac{\eta^2}{(1+q)} \left[(1 + B_H \eta) (\alpha_2^{\parallel} - q \alpha_1^{\parallel}) \right. \\ &\quad \left. + H_S \frac{(1-q)}{(1+q)^2} (\alpha_2^{\parallel} + q^2 \alpha_1^{\parallel}) \right], \\ v_{\parallel} &= K \frac{\eta^2}{(1+q)} \left[(1 + B_K \eta) |\alpha_2^{\perp} - q \alpha_1^{\perp}| \right. \\ &\quad \times \cos(\Theta_{\Delta} - \Theta_0) \\ &\quad \left. + K_S \frac{(1-q)}{(1+q)^2} |\alpha_2^{\perp} + q^2 \alpha_1^{\perp}| \right. \\ &\quad \left. \times \cos(\Theta_S - \Theta_1) \right], \end{aligned} \quad (1)$$

where $\eta = q/(1+q)^2$, with $q = m_1/m_2$ the mass ratio of the smaller to larger mass hole, $\vec{\alpha}_i = \vec{S}_i/m_i^2$, the

index \perp and \parallel refer to perpendicular and parallel to the orbital angular momentum respectively, \hat{e}_1, \hat{e}_2 are orthogonal unit vectors in the orbital plane, and ξ measures the angle between the unequal mass and spin contribution to the recoil velocity in the orbital plane. from newly available runs. The angle Θ is defined as the angle between the in-plane component of $\vec{\Delta} = M(\vec{S}_2/m_2 - \vec{S}_1/m_1)$ or $\vec{S} = \vec{S}_1 + \vec{S}_2$ and a fiducial direction at merger (see Ref. [18] technique). Phases Θ_0 and Θ_1 depend on the initial separation of the holes for quasicircular orbits (astrophysically realistic evolutions of comparable masses black holes lead to nearly zero eccentricity mergers).

The empirical formula (1) above was obtained by assuming the post-Newtonian dependence on the spin and mass ratio of instantaneous radiated linear momenta [69] where the coefficients are to be fitted by full numerical simulations. Second order corrections in the spin have been obtained recently [70] and could be added to the empirical formula. Here, in this paper, we will consider instead the particular family of configurations that lead to the maximum recoil [15–17, 71], where $q = 1$ and the two spins are in the orbital plane, equal in magnitude, and opposite in direction. These configurations are π -symmetric, i.e. rotating the system by 180 degrees around the symmetry axis lead to the same configuration. This implies in particular, that only odd powers of the spin and the $\cos \Theta$ are involved. We will then perform a series of simulations that vary both the magnitude of the (intrinsic) spin in the range $\alpha = 0.2 - 0.92$ and the initial angle of the individual black-hole spin and orbital linear momentum.

For a first exploration of the extended spin dependence we consider cubic and possible fifth-order corrections [32] to the empirical formula (1) of the form

$$v_{\parallel} = (V_{1,1}\alpha + V_{1,3}\alpha^3) \cos(\Theta_{\Delta} - \Theta_0) + (V_{3,1}\alpha + V_{3,3}\alpha^3 + V_{3,5}\alpha^5) \cos(3\Theta_{\Delta} - 3\Theta_3), \quad (2)$$

where $V_{1,1} = 2K(1+\eta B_K) \frac{\eta^2}{(1+q)}$, and the remaining terms are higher-order correction to Eq. (1).

II. TECHNIQUES

To compute the numerical initial data, we use the puncture approach [72] along with the TWOPUNCTURES [73] thorn. In this approach the 3-metric on the initial slice has the form $\gamma_{ab} = (\psi_{BL} + u)^4 \delta_{ab}$, where ψ_{BL} is the Brill-Lindquist conformal factor, δ_{ab} is the Euclidean metric, and u is (at least) C^2 on the punctures. The Brill-Lindquist conformal factor is given by $\psi_{BL} = 1 + \sum_{i=1}^n m_i^p / (2|\vec{r} - \vec{r}_i|)$, where n is the total number of ‘punctures’, m_i^p is the mass parameter of puncture i (m_i^p is *not* the horizon mass associated with puncture i), and \vec{r}_i is the coordinate location of puncture i . For the initial (conformal) extrinsic curvature we take the analytic form \hat{K}_{ij}^{BY} given by Bowen and York[74]. We evolve

these black-hole-binary data-sets using the LAZEV [75] implementation of the moving puncture formalism [1, 2] with the conformal factor $W = \sqrt{\chi} = \exp(-2\phi)$ suggested by [4] as a dynamical variable. For the runs presented here we use centered, eighth-order finite differencing in space [76] and an RK4 time integrator (note that we do not upwind the advection terms).

We use the Carpet [77] mesh refinement driver to provide a ‘moving boxes’ style mesh refinement. In this approach refined grids of fixed size are arranged about the coordinate centers of both holes. The Carpet code then moves these fine grids about the computational domain by following the trajectories of the two black holes.

We use AHFINDERDIRECT [78] to locate apparent horizons. We measure the magnitude of the horizon spin using the Isolated Horizon algorithm detailed in [79]. This algorithm is based on finding an approximate rotational Killing vector (i.e. an approximate rotational symmetry) on the horizon φ^a . Given this approximate Killing vector φ^a , the spin magnitude is

$$S_{[\varphi]} = \frac{1}{8\pi} \int_{AH} (\varphi^a R^b K_{ab}) d^2V, \quad (3)$$

where K_{ab} is the extrinsic curvature of the 3D-slice, d^2V is the natural volume element intrinsic to the horizon, and R^a is the outward pointing unit vector normal to the horizon on the 3D-slice. We measure the direction of the spin by finding the coordinate line joining the poles of this Killing vector field using the technique introduced in [5]. Our algorithm for finding the poles of the Killing vector field has an accuracy of $\sim 2^\circ$ (see [5] for details). Note that once we have the horizon spin, we can calculate the horizon mass via the Christodoulou formula

$$m^H = \sqrt{m_{\text{irr}}^2 + S^2/(4m_{\text{irr}}^2)}, \quad (4)$$

where $m_{\text{irr}} = \sqrt{A/(16\pi)}$ and A is the surface area of the horizon. We measure radiated energy, linear momentum, and angular momentum, in terms of ψ_4 , using the formulae provided in Refs. [80, 81]. However, rather than using the full ψ_4 , we decompose it into ℓ and m modes and solve for the radiated linear momentum, dropping terms with $\ell \geq 5$. The formulae in Refs. [80, 81] are valid at $r = \infty$. We obtain highly accurate values for these quantities by solving for them on spheres of finite radius (typically $r/M = 50, 60, \dots, 100$), fitting the results to a polynomial dependence in $l = 1/r$, and extrapolating to $l = 0$ [2, 38, 82, 83]. Each quantity Q has the radial dependence $Q = Q_0 + lQ_1 + \mathcal{O}(l^2)$, where Q_0 is the asymptotic value (the $\mathcal{O}(l)$ error arises from the $\mathcal{O}(l)$ error in $r\psi_4$). We perform both linear and quadratic fits of Q versus l , and take Q_0 from the quadratic fit as the final value with the differences between the linear and extrapolated Q_0 as a measure of the error in the extrapolations.

We obtain accurate, convergent waveforms and horizon parameters by evolving this system in conjunction with a modified 1+log lapse and a modified Gamma-driver

shift condition [1, 84], and an initial lapse $\alpha(t = 0) = 2/(1 + \psi_{BL}^4)$. The lapse and shift are evolved with

$$(\partial_t - \beta^i \partial_i) \alpha = -2\alpha K, \quad (5a)$$

$$\partial_t \beta^a = (3/4) \bar{\Gamma}^a - \eta(x^a, t) \beta^a, \quad (5b)$$

where different functional dependences for $\eta(x^a, t)$ have been proposed in [75, 85–89]. For the low-spin simulations we used a constant $\eta = 2$, while for the $\alpha = 0.92$ simulation we used a modification of the form proposed in [90],

$$\eta(x^a, t) = R_0 \frac{\sqrt{\bar{\gamma}^{ij} \partial_i W \partial_j W}}{(1 - W^a)^b}, \quad (6)$$

where we chose $R_0 = 1.31$ [86]. In practice we used $a = 2$ and $b = 2$, which reduces η by a factor of 4 at infinity when compared to the gauge proposed by [86], improving its stability at larger radii. Other values of (a, b) lead to an increase of the numerical noise. Note that this gauge was originally proposed and used for the non-spinning, intermediate-mass-ratio binaries. Here we find that the gauge is well adapted for the highly-spinning equal mass case, where, after the initial burst of radiation passes, the measured spin is found to never drop below $\alpha = 0.905$. Due to the differences in the spurious initial radiation content, as well as spin-orbit effects on the total mass, α near merger varied from between 0.90 to 0.93 for the different A09Tyyy configurations (See tables I and II below).

A. Initial Data

We used 3PN parameters for quasicircular orbits with BH spins (equal in magnitude and opposite in direction) aligned with the linear momentum of each BH (i.e. in-plane spins) to obtain the momenta and spin parameters for the Bowen-York extrinsic curvature. We then chose puncture mass parameters such that the total ADM mass was 1M. We then rotated the spins by 30° , 90° , 130° , 210°

and 315° , to obtain a total of 6 configurations for each value of the intrinsic spin α . We label the configuration AxxTyyy where xx corresponds to the spin of each BH and yyy is the initial rotation of the spin directions. We summarize the initial data in Table I.

This family of configurations has larger initial separations than the configurations in our original studies in [16]. In these configurations, the BHs orbit ~ 3.5 times prior to merger, which allows for most of the eccentricity to be radiated away before the plunge phase (where most of the recoil velocity is generated). This provides for an accurate description of the plausible astrophysical maximal recoil scenario.

TABLE I: Initial data parameters for the non-rotated configurations. The initial puncture positions are $\pm(x, 0, 0)$, momenta are $\pm(0, p, 0)$, and spin $\pm(0, S, 0)$. The remaining configurations are obtained by rotating the spins, keeping all other parameters the same.

Config	x	p	S	m_p
A02T000	3.878113	0.117404	0.051314	0.479782
A04T000	3.879566	0.117405	0.102627	0.454076
A06T000	3.881979	0.117407	0.153936	0.403550
A08T000	3.885342	0.117409	0.205241	0.301026
A09T000	3.887375	0.117411	0.230891	0.172120

III. RESULTS AND ANALYSIS

In order to analyze our results for different initial orientations of the spin that span the Θ -dependence, we use the techniques detailed in [18]. For each α we fit the results of the recoil as a function of angle to form $V_{\text{recoil}} = V_1 \cos(\theta - \theta_1) + V_3 \cos[3(\theta - \theta_3)]$, where θ is defined to be the angle of the spin direction (of the first BH) near merger (at a fiducial radial separation of $r = 1.2$) and the spin direction of the corresponding AxxT000 configuration (we cannot simply use the initial spin direction differences because spin-orbit effects for larger spins make this approximation inaccurate). The radiated energy and recoil from each simulation is given in Table II.

We then fit V_1 and V_3 to the functional forms $V_1 = V_{1,1}\alpha + V_{1,3}\alpha^3$ and $V_3 = V_{3,1}\alpha + V_{3,3}\alpha^3$. A summary of the fits is given in Table III. Note that $V_{1,1}$ is related to the parameter K in our empirical formula (2) by $K = 16V_{1,1}$. Here we find $K = 58912 \pm 43$, where the error is obtained from the fit and likely underestimated the true error in this quantity. Previously we found $K = (6.0 \pm 0.1) \times 10^4$, which agrees reasonably well with the new value [16, 18]. We also include fits where the linear term in V_3 and the cubic term in V_1 are set to zero, as well as a fit of V_3 to $V_{3,3}\alpha^3 + V_{3,5}\alpha^5$. We note that a cubic term in V_1 is expected since $\cos^3 \theta = 3/4 \cos \theta + 1/3 \cos 3\theta$, and hence cubic corrections of the form $\alpha^3 \cos^3 \theta$ will contribute to

the $\cos \theta$ dependence. On the other hand, a linear dependence in $\cos 3\theta$ is not expected.

The form of the fitting above was first proposed in [32] as a generic expansion, where it was applied to data sets with constant α . Here we compare results from five different values of the intrinsic spin in the range $\alpha = 0.2 - 0.92$, to obtain an accurate model of the α dependence.

In Figs. 1-5 we show the angular fits for each set of configurations. Note that the spin-orbit coupling effects are strongest for the A09Tyyy configurations, as is apparent by the relative translation of two configurations towards the same final angle.

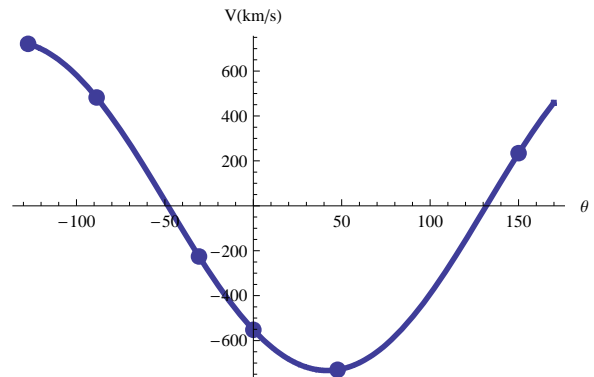
TABLE II: The radiated energy, recoil velocity, and angle between the spins for the AxxTyyy configuration at merger and the corresponding AxxT000 configuration, $\Delta\Theta$. Note the substantial rotations apparent in the A09Tyyy configurations due to spin orbit interactions.

Config	δE	V_{recoil}	$\Delta\Theta$	δJ_z
A02T000	0.03583 ± 0.00020	551.95 ± 0.83	0	0.2727 ± 0.0032
A02T030	0.03575 ± 0.00020	225.49 ± 0.86	30.7	0.2724 ± 0.0031
A02T090	0.03562 ± 0.00019	-482.10 ± 0.13	88.6	0.2721 ± 0.0031
A02T130	0.03574 ± 0.00019	-721.03 ± 0.34	127.3	0.2727 ± 0.0031
A02T210	0.03573 ± 0.00020	-234.14 ± 0.76	210.0	0.2723 ± 0.0032
A02T315	0.03577 ± 0.00019	730.10 ± 0.32	312.4	0.2729 ± 0.0030
A04T000	0.03665 ± 0.00022	1200.79 ± 2.21	0	0.2768 ± 0.0031
A04T030	0.03625 ± 0.00022	529.09 ± 2.12	33.7	0.2747 ± 0.0031
A04T090	0.03574 ± 0.00020	-764.08 ± 0.39	85.0	0.2740 ± 0.0028
A04T130	0.03620 ± 0.00021	-1390.22 ± 0.89	126.0	0.2759 ± 0.0029
A04T210	0.03633 ± 0.00021	-637.049 ± 1.97	209.2	0.2755 ± 0.0030
A04T315	0.03628 ± 0.00021	1424.17 ± 1.02	311.2	0.2762 ± 0.0029
A06T000	0.03803 ± 0.00027	2001.06 ± 3.5	0	0.2834 ± 0.0032
A06T030	0.03740 ± 0.00026	1087.24 ± 4.8	36.2	0.2798 ± 0.0032
A06T090	0.03595 ± 0.00025	-870.93 ± 2.4	87.3	0.2758 ± 0.0026
A06T130	0.03669 ± 0.00026	-1944.04 ± 1.5	127.7	0.2791 ± 0.0029
A06T210	0.03751 ± 0.00026	-1212.62 ± 4.4	212.4	0.2807 ± 0.0031
A06T315	0.03679 ± 0.00026	1984.74 ± 1.3	310.3	0.2797 ± 0.0029
A08T000	0.03996 ± 0.00039	2651.75 ± 7.54	0	0.2912 ± 0.0027
A08T030	0.03941 ± 0.00037	1917.03 ± 8.29	24.3	0.2888 ± 0.0027
A08T090	0.03677 ± 0.00034	-445.83 ± 1.10	70.9	0.2791 ± 0.0028
A08T130	0.03733 ± 0.00038	-2412.2 ± 4.03	119.5	0.2823 ± 0.0027
A08T210	0.03941 ± 0.00036	-1919.86 ± 8.26	204.3	0.2887 ± 0.0027
A08T315	0.03771 ± 0.00038	2568.87 ± 4.49	306.3	0.2838 ± 0.0027
A09T000	0.04026 ± 0.00057	89.74 ± 1.00	0	0.3063 ± 0.0042
A09T030	0.04143 ± 0.00055	3240.96 ± 17.34	101.5	0.3011 ± 0.0051
A09T090	0.04062 ± 0.00057	1859.42 ± 15.47	147.4	0.2951 ± 0.0070
A09T130	0.03784 ± 0.00054	-759.16 ± 0.85	190.6	0.2846 ± 0.0058
A09T210	0.04144 ± 0.00055	-3239.25 ± 17.24	281.7	0.3012 ± 0.0050
A09T315	0.03917 ± 0.00056	-205.59 ± 2.92	355.3	0.2919 ± 0.0067

In Table III we provide the fitting constants $V_{i,j}$ assuming the spin of the A09Tyyy was 0.92. In actuality, the spin varied between configurations. In Table IV we provide fitting parameters for $V_{i,j}$ if we take the value of α for these configurations to be $\alpha = 0.9$ (the expected value when neglecting effects due to the initial radiation content), $\alpha = 0.91$, and $\alpha = 0.92$ (which approximates the average value of α over all configurations). We find that setting $\alpha = 0.92$ gives the best fit for the dominant $V_{1,1}$ term. However, we note that these fits do indicate that the nonleading $V_{1,3}$ term and $V_{3,1}$ term may be zero. We therefore also provide fits assuming these two terms vanish. Fits to V_1 strongly prefer $\alpha = 0.92$ over the smaller values. We note that the sign of $V_{1,3}$ changes if we assume smaller values of α for the A09Tyyy configurations.

While arguments based on post-Newtonian scaling do not seem to indicate the presence of an $\alpha \cos 3\Theta$ term, our results indicate that this term is present. This may indicate an error in V_3 for $\alpha = 0.2$. If we exclude this data point, then we can fit to reasonably well to either $V_{3,1}\alpha + V_{3,3}\alpha^3$ or $V_{3,3}\alpha^3 + V_{3,5}\alpha^5$. Further exploration in the small α regime is required. In Figs 6 we compare fits

FIG. 1: Fit of the recoil versus angle for the $\alpha = 0.2$ configurations.



of V_3 and find that the best fit is to $V_3 = \alpha V_{3,1} + \alpha^3 V_{3,3}$. On the other hand, as seen in Fig. 7, there is no significant difference apparent in the fits of V_1 to $V_{1,1}\alpha + V_{1,3}\alpha^3$ and $V_1 = V_{1,1}\alpha$.

TABLE III: Fits of the recoil to the functional form $v_{\text{kick}} = V_1 \cos(\theta - \theta_1) + V_3 \cos[3(\theta - \theta_3)]$. Note that angles are measured in degrees. The reported errors come from the nonlinear least-squares fit of the data and are underestimates of the actual errors. Note the average value of α for the A09Tyyy configuration near merger was $\alpha \sim 0.92$, which was the value used to obtain the fits to $V_{i,j}$.

α	V_1	θ_1
0	0	****
0.2	737.70 ± 0.12	221.8002 ± 0.0010
0.4	1472.59 ± 0.06	215.6909 ± 0.0011
0.6	2204.98 ± 0.56	205.117 ± 0.015
0.8	2935.93 ± 0.65	206.658 ± 0.013
0.9	3376.3 ± 7.5	91.02 ± 0.11
α	V_3	θ_3
0 0	****	
0.2	4.23 ± 0.12	279.62 ± 0.65
0.4	12.0838 ± 0.024	37.790 ± 0.049
0.6	31.63 ± 0.55	152.72 ± 0.38
0.8	69.21 ± 0.74	38.01 ± 0.22
0.9	95.5 ± 2.4	36.7 ± 1.5
$V_{1,1}$	3681.77 ± 2.66	
$V_{1,3}$	-15.46 ± 3.97	
$V_{3,1}$	15.65 ± 3.01	
$V_{3,3}$	105.90 ± 4.50	

TABLE IV: Fits V_1 and V_3 to the form $V_1 = V_{1,1}\alpha + V_{1,3}\alpha^3$ and $V_3 = V_{3,1}\alpha + V_{3,3}\alpha^3$, as well as $V_3 = V_{3,3}\alpha^3 + V_{3,5}\alpha^5$. For the A09Tyyy configurations we take $\alpha = 0.9, 0.91, \text{ and } 0.92$, which accounts for the expected value of α for these configuration, the actual average value observed, and a spin between these two values, as explained in the text. δ^2 is the average of the square of the error in the fit. Note that fits to the dominant V_1 term strongly prefer $\alpha = 0.92$ over smaller values, while fits to the subleading V_3 prefer $\alpha = 0.9$.

α (A09Tyyy)	$V_{1,1}$	$V_{1,3}$	δ^2
0.92	3681.77 ± 2.66	-15.46 ± 3.966	1.21
0.91	3658.21 ± 20.74	49.16, 31.47	71.13
0.90	3634.85 ± 41.09	115.31, 63.40	270.25
α (A09Tyyy)	$V_{3,1}$	$V_{3,3}$	δ^2
0.92	15.65 ± 3.01	105.90 ± 4.50	1.55
0.91	13.68 ± 1.82	111.15 ± 2.77	0.55
0.90	11.75 ± 1.14	116.45 ± 1.77	0.21
α (A09Tyyy)	$V_{1,1}$		δ^2
0.92	3672.08 ± 1.84	0	5.80
0.91	3688.56 ± 8.23	0	114.53
0.90	3704.98 ± 17.17	0	493.78
α (A09Tyyy)		$V_{3,3}$	δ^2
0.92	0	127.74 ± 3.96	12.02
0.91	0	130.60 ± 3.36	8.29
0.90	0	133.45 ± 2.90	5.73
α (A09Tyyy)	$V_{3,3}$	$V_{3,5}$	δ^2
0.92	172.55 ± 10.20	-58.98 ± 13.21	2.01
0.91	167.45 ± 10.87	-49.54 ± 14.38	2.09
0.90	161.80 ± 12.15	-38.88 ± 16.43	2.389

FIG. 2: Fit of the recoil versus angle for the $\alpha = 0.4$ configurations.

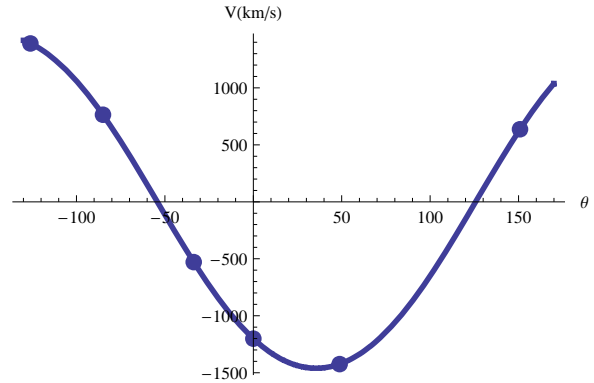
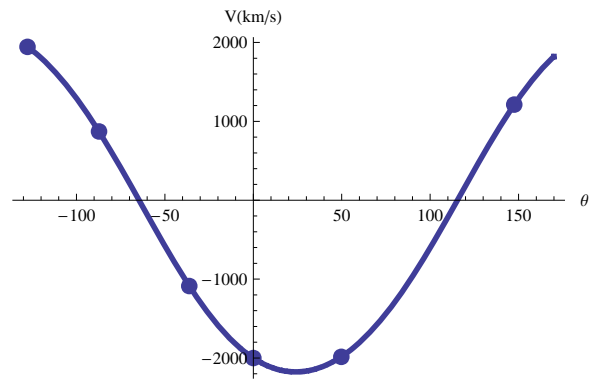


FIG. 3: Fit of the recoil versus angle for the $\alpha = 0.6$ configurations.



IV. CONCLUSION

Using the enhanced recoil formula for the “maximum kick” configurations, we predict that the maximum recoil will be $3680 \pm 130 \text{ km s}^{-1}$, where the error in the prediction is due to the possibility of the higher-order effects producing recoils in the same direction or opposite direction of the dominant linear contribution. We

FIG. 4: Fit of the recoil versus angle for the $\alpha = 0.8$ configurations.

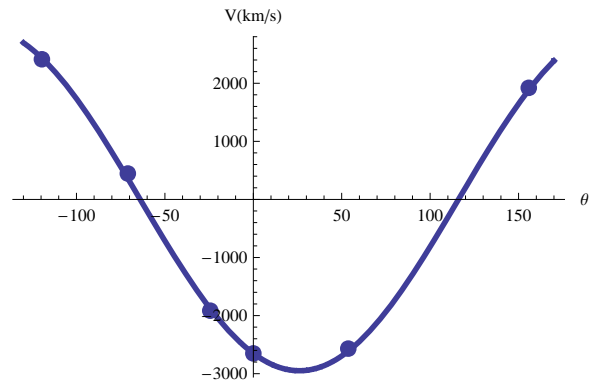


FIG. 5: Fit of the recoil versus angle for the $\alpha = 0.92$ configurations.

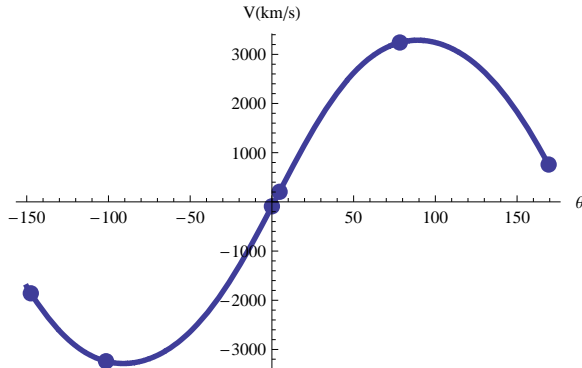
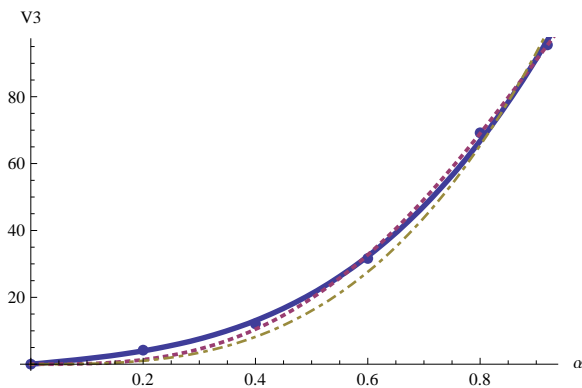


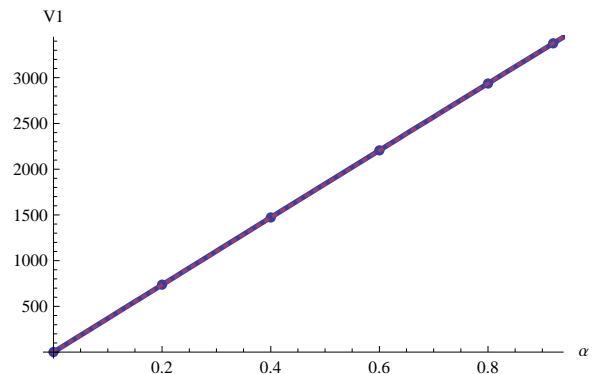
FIG. 6: A comparison of fits of V_3 to $V_3 = \alpha V_{3,1} + \alpha^3 V_{3,3}$ (solid), $V_3 = \alpha^3 V_{3,3} + \alpha^5 V_{3,5}$ (dotted), $V_3 = \alpha^3 V_{3,3}$ (dot-dashed). The first fit is the best. In all cases the spins for the A09Tyyy configurations were assumed to be $\alpha = 0.92$



also established a model for higher-order dependences on the spin in the recoil formula. These results are particularly relevant for the interpretation of observations of emission lines in AGNs displaying displacements between narrow and wide emission lines of the order of thousands of kilometers per second. In particular in Ref. [91] a 1200 km/s offset velocity was measured (CXOCJ100043.1+020637). A 2650 km/s recoil-

ing supermassive black hole could explain the observations (SDSS J092712+294344) of Ref. [60]. While in Ref. [62] (SDSS J105041+345631) and in Ref. [92] (SDSS J153636+044127) there is speculation that 3500 km/s recoiling black holes are responsible for these features in the spectra. While none of those cases effectively surpasses the maximum recoil velocity determined here, they came close enough for the probability of actually observing this event to be very low [93] thus leading to the question about what are the astrophysical mechanisms responsible of generating such large differential velocities [94, 95].

FIG. 7: A comparison of fits of V_1 to $V_1 = \alpha V_{1,1} + \alpha^3 V_{1,3}$ (solid), $V_3 = \alpha V_{1,1}$ (dotted). There is no significant differences between the fits. In all cases the spins for the A09Tyyy configurations were assumed to be $\alpha = 0.92$



Acknowledgments

We gratefully acknowledge the NSF for financial support from Grants No. PHY-0722315, No. PHY-0653303, No. PHY-0714388, No. PHY-0722703, No. DMS-0820923, No. PHY-0929114, No. PHY-0969855, No. PHY-0903782, No. CDI-1028087; and NASA for financial support from NASA Grants No. 07-ATFP07-0158 and No. HST-AR-11763. Computational resources were provided by the Ranger cluster at TACC (Teragrid allocation TG-PHY060027N) and by NewHorizons at RIT.

-
- [1] M. Campanelli, C. O. Lousto, P. Marronetti, and Y. Zlochower, Phys. Rev. Lett. **96**, 111101 (2006), gr-qc/0511048.
 - [2] J. G. Baker, J. Centrella, D.-I. Choi, M. Koppitz, and J. van Meter, Phys. Rev. Lett. **96**, 111102 (2006), gr-qc/0511103.
 - [3] F. Pretorius, Phys. Rev. Lett. **95**, 121101 (2005), gr-qc/0507014.
 - [4] P. Marronetti, W. Tichy, B. Brugmann, J. Gonzalez, and U. Sperhake, Phys. Rev. **D77**, 064010 (2008), 0709.2160.
 - [5] M. Campanelli, C. O. Lousto, Y. Zlochower, B. Krishnan, and D. Merritt, Phys. Rev. **D75**, 064030 (2007), gr-qc/0612076.
 - [6] M. Campanelli, C. O. Lousto, and Y. Zlochower, Phys. Rev. D **74**, 041501(R) (2006), gr-qc/0604012.
 - [7] M. Campanelli, C. O. Lousto, and Y. Zlochower, Phys. Rev. D **74**, 084023 (2006), astro-ph/0608275.
 - [8] F. Herrmann, I. Hinder, D. M. Shoemaker, P. Laguna, and R. A. Matzner, Phys. Rev. **D76**, 084032 (2007), 0706.2541.
 - [9] P. Marronetti et al., Class. Quant. Grav. **24**, S43 (2007), gr-qc/0701123.
 - [10] E. Berti et al., Phys. Rev. **D76**, 064034 (2007), gr-qc/0703053.
 - [11] F. Herrmann, I. Hinder, D. Shoemaker, P. Laguna, and R. A. Matzner, Astrophys. J. **661**, 430 (2007), gr-

- qc/0701143.
- [12] F. Herrmann, D. Shoemaker, and P. Laguna, AIP Conf. **873**, 89 (2006), gr-qc/0601026.
- [13] J. G. Baker et al., *Astrophys. J.* **653**, L93 (2006), astro-ph/0603204.
- [14] J. A. González, U. Sperhake, B. Bruggmann, M. Hannam, and S. Husa, *Phys. Rev. Lett.* **98**, 091101 (2007), gr-qc/0610154.
- [15] M. Campanelli, C. O. Lousto, Y. Zlochower, and D. Merritt, *Astrophys. J.* **659**, L5 (2007), gr-qc/0701164.
- [16] M. Campanelli, C. O. Lousto, Y. Zlochower, and D. Merritt, *Phys. Rev. Lett.* **98**, 231102 (2007), gr-qc/0702133.
- [17] J. A. González, M. D. Hannam, U. Sperhake, B. Bruggmann, and S. Husa, *Phys. Rev. Lett.* **98**, 231101 (2007), gr-qc/0702052.
- [18] C. O. Lousto and Y. Zlochower, *Phys. Rev. D* **79**, 064018 (2009), 0805.0159.
- [19] D. Pollney et al., *Phys. Rev.* **D76**, 124002 (2007), 0707.2559.
- [20] B. Bruggmann, J. A. Gonzalez, M. Hannam, S. Husa, and U. Sperhake, *Phys. Rev.* **D77**, 124047 (2008), 0707.0135.
- [21] D.-I. Choi et al., *Phys. Rev.* **D76**, 104026 (2007), gr-qc/0702016.
- [22] J. G. Baker et al., *Astrophys. J.* **668**, 1140 (2007), astro-ph/0702390.
- [23] J. D. Schnittman et al., *Phys. Rev.* **D77**, 044031 (2008), 0707.0301.
- [24] J. G. Baker et al., *Astrophys. J.* **682**, L29 (2008), 0802.0416.
- [25] J. Healy et al., *Phys. Rev. Lett.* **102**, 041101 (2009), 0807.3292.
- [26] F. Herrmann, I. Hinder, D. Shoemaker, and P. Laguna, *Class. Quant. Grav.* **24**, S33 (2007).
- [27] W. Tichy and P. Marronetti, *Phys. Rev.* **D76**, 061502 (2007), gr-qc/0703075.
- [28] M. Koppitz et al., *Phys. Rev. Lett.* **99**, 041102 (2007), gr-qc/0701163.
- [29] S. H. Miller and R. A. Matzner, *Gen. Rel. Grav.* **41**, 525 (2009), 0807.3028.
- [30] C. O. Lousto, M. Campanelli, Y. Zlochower, and H. Nakano, *Class. Quant. Grav.* **27**, 114006 (2010), 0904.3541.
- [31] L. Boyle, M. Kesden, and S. Nissanke, *Phys. Rev. Lett.* **100**, 151101 (2008), 0709.0299.
- [32] L. Boyle and M. Kesden, *Phys. Rev.* **D78**, 024017 (2008), 0712.2819.
- [33] A. Buonanno, L. E. Kidder, and L. Lehner, *Phys. Rev.* **D77**, 026004 (2008), arXiv:0709.3839 [astro-ph].
- [34] W. Tichy and P. Marronetti, *Phys. Rev.* **D78**, 081501 (2008), 0807.2985.
- [35] M. Kesden, *Phys. Rev.* **D78**, 084030 (2008), 0807.3043.
- [36] E. Barausse and L. Rezzolla, *Astrophys. J. Lett.* **704**, L40 (2009), 0904.2577.
- [37] L. Rezzolla, *Class. Quant. Grav.* **26**, 094023 (2009), 0812.2325.
- [38] M. Hannam, S. Husa, U. Sperhake, B. Bruggmann, and J. A. Gonzalez, *Phys. Rev.* **D77**, 044020 (2008), 0706.1305.
- [39] A. Buonanno, G. B. Cook, and F. Pretorius, *Phys. Rev.* **D75**, 124018 (2007), gr-qc/0610122.
- [40] J. G. Baker, J. R. van Meter, S. T. McWilliams, J. Centrella, and B. J. Kelly, *Phys. Rev. Lett.* **99**, 181101 (2007), gr-qc/0612024.
- [41] Y. Pan et al., *Phys. Rev.* **D77**, 024014 (2008), arXiv:0704.1964 [gr-qc].
- [42] A. Buonanno et al., *Phys. Rev.* **D76**, 104049 (2007), arXiv:0706.3732 [gr-qc].
- [43] M. Hannam, S. Husa, B. Bruggmann, and A. Gopakumar, *Phys. Rev.* **D78**, 104007 (2008), 0712.3787.
- [44] A. Gopakumar, M. Hannam, S. Husa, and B. Bruggmann, *Phys. Rev.* **D78**, 064026 (2008), 0712.3737.
- [45] I. Hinder, F. Herrmann, P. Laguna, and D. Shoemaker, *Phys. Rev.* **D82**, 024033 (2010), 0806.1037.
- [46] Z. Haiman, B. Kocsis, K. Menou, Z. Lippai, and Z. Frei, *Class. Quant. Grav.* **26**, 094032 (2009), 0811.1920.
- [47] G. A. Shields and E. W. Bonning, *Astrophys. J.* **682**, 758 (2008), 0802.3873.
- [48] Z. Lippai, Z. Frei, and Z. Haiman, *Astrophys. J. Lett.* **676**, L5 (2008), 0801.0739.
- [49] G. A. Shields, E. W. Bonning, and S. Salviander, in *Space Telescope Science Institute Symposium: Black Holes* (2007), 0707.3625.
- [50] S. Komossa and D. Merritt, *Astrophys. J.* **683**, L21 (2008), 0807.0223.
- [51] E. W. Bonning, G. A. Shields, and S. Salviander, *apjl* **666**, L13 (2007), 0705.4263.
- [52] A. Loeb, *Phys. Rev. Lett.* **99**, 041103 (2007), astro-ph/0703722.
- [53] J. D. Schnittman and J. H. Krolik, *Astrophys. J.* **684**, 835 (2008), 0802.3556.
- [54] B. Devecchi, M. Dotti, E. Rasia, M. Volonteri, and M. Colpi, *Mon. Not. Roy. Astron. Soc.* **394**, 633 (2009), 0805.2609.
- [55] Y. Fujita, *Astrophys. J.* **691**, 1050 (2009), 0810.1520.
- [56] Y. Fujita, *Astrophys. J. Lett.* **685**, L59 (2008), 0808.1726.
- [57] S. Komossa and D. Merritt, *Astrophys. J. Lett.* **689**, 189 (2008), 0811.1037.
- [58] D. Merritt, J. D. Schnittman, and S. Komossa, *Astrophys. J.* **699**, 1690 (2009), 0809.5046.
- [59] M. Volonteri and P. Madau, *Astrophys. J.* **687**, L57 (2008), 0809.4007.
- [60] S. Komossa, H. Zhou, and H. Lu, *Astrop. J. Letters* **678**, L81 (2008), 0804.4585.
- [61] I. V. Strateva and S. Komossa, *Astrophys. J.* **692**, 443 (2009), 0810.3793.
- [62] G. Shields, D. Rosario, K. Smith, E. Bonning, S. Salviander, et al., *Astrophys. J.* **707**, 936 (2009), arXiv:0907.3470.
- [63] T. M. Heckman, J. H. Krolik, S. M. Moran, J. Schnittman, and S. Gezari, *Astrophys. J.* **695**, 363 (2009), 0810.1244.
- [64] G. A. Shields, E. W. Bonning, and S. Salviander, *Astrophys. J.* **696**, 1367 (2009), 0810.2563.
- [65] T. Bogdanovic, M. Eracleous, and S. Sigurdsson, *Astrophys. J.* **697**, 288 (2009), 0809.3262.
- [66] M. Dotti et al., *Mon. Not. Roy. Astron. Soc.* **398**, L73 (2009), 0809.3446.
- [67] C. O. Lousto and Y. Zlochower (2010), 1009.0292.
- [68] G. Lovelace, M. A. Scheel, and B. Szilagyi (2010), 1010.2777.
- [69] L. E. Kidder, *Phys. Rev. D* **52**, 821 (1995), gr-qc/9506022.
- [70] E. Racine, A. Buonanno, and L. E. Kidder, *Phys. Rev.* **D80**, 044010 (2009), 0812.4413.
- [71] S. Dain, C. O. Lousto, and Y. Zlochower, *Phys. Rev. D* **78**, 024039 (2008), 0803.0351.
- [72] S. Brandt and B. Bruggmann, *Phys. Rev. Lett.* **78**, 3606

- (1997), gr-qc/9703066.
- [73] M. Ansorg, B. Brügmann, and W. Tichy, *Phys. Rev. D* **70**, 064011 (2004), gr-qc/0404056.
- [74] J. M. Bowen and J. W. York, Jr., *Phys. Rev. D* **21**, 2047 (1980).
- [75] Y. Zlochower, J. G. Baker, M. Campanelli, and C. O. Lousto, *Phys. Rev. D* **72**, 024021 (2005), gr-qc/0505055.
- [76] C. O. Lousto and Y. Zlochower, *Phys. Rev.* **D77**, 024034 (2008), 0711.1165.
- [77] E. Schnetter, S. H. Hawley, and I. Hawke, *Class. Quantum Grav.* **21**, 1465 (2004), gr-qc/0310042.
- [78] J. Thornburg, *Class. Quantum Grav.* **21**, 743 (2004), gr-qc/0306056.
- [79] O. Dreyer, B. Krishnan, D. Shoemaker, and E. Schnetter, *Phys. Rev. D* **67**, 024018 (2003), gr-qc/0206008.
- [80] M. Campanelli and C. O. Lousto, *Phys. Rev. D* **59**, 124022 (1999), gr-qc/9811019.
- [81] C. O. Lousto and Y. Zlochower, *Phys. Rev. D* **76**, 041502(R) (2007), gr-qc/0703061.
- [82] M. Campanelli, C. O. Lousto, and Y. Zlochower, *Phys. Rev. D* **73**, 061501(R) (2006).
- [83] M. Boyle et al., *Phys. Rev.* **D76**, 124038 (2007), arXiv:0710.0158 [gr-qc].
- [84] M. Alcubierre, B. Brügmann, P. Diener, M. Koppitz, D. Pollney, E. Seidel, and R. Takahashi, *Phys. Rev. D* **67**, 084023 (2003), gr-qc/0206072.
- [85] M. Alcubierre et al. (2004), gr-qc/0411137.
- [86] D. Mueller and B. Bruegmann, *Class. Quant. Grav.* **27**, 114008 (2010), 0912.3125.
- [87] D. Mueller, J. Grigsby, and B. Bruegmann, *Phys. Rev.* **D82**, 064004 (2010), 1003.4681.
- [88] E. Schnetter, *Class. Quant. Grav.* **27**, 167001 (2010), 1003.0859.
- [89] D. Alic, L. Rezzolla, I. Hinder, and P. Mosta (2010), 1008.2212.
- [90] C. O. Lousto, H. Nakano, Y. Zlochower, and M. Campanelli (2010), 1008.4360.
- [91] F. Civano et al., *Astrophys. J.* **717**, 209 (2010), 1003.0020.
- [92] T. A. Boroson and T. R. Lauer, *Nature (London)* **458**, 53 (2009), 0901.3779.
- [93] C. O. Lousto, H. Nakano, Y. Zlochower, and M. Campanelli, *Phys. Rev.* **D81**, 084023 (2010), 0910.3197.
- [94] M. Vivek, R. Srianand, P. Noterdaeme, V. Mohan, and V. Kuriakose, *mnras* **400**, L6 (2009), arXiv:0909.0018.
- [95] T. R. Lauer and T. A. Boroson, *Astrophys. J.* **703**, 930 (2009), arXiv:0906.0020.